EFFECT OF SURFACTANT ON FABRICATION OF CORE-SHELL STRUCTURED MESOPOROUS SILICA NANOPARTICLES

Ngoc Huyen Nguyen Thi[1], Xuan Thi Diem Trinh Nguyen[1],

Nguyen Minh Thao[2], Ngoc Tram Nguyen Thi[1,*]

[1]*College of Medicine and Pharmacy, Tra Vinh University, Vietnam*

[2]*Department of Science and Technology, Dong Thap University, Vietnam*

Email: tram06@tvu.edu.vn

ABSTRACT

Hollow mesoporous silica nanoparticles (HMSN) were synthesized by the hard-template method, consisting of three stages: forming a solid silica nano core (SSN), developing a core-shell structure **(SSN@CTAB-SSN),** and etching the core to form hollow silica nanoparticles. This study evaluated the effect of surfactant (Cetyltrimethylammonium Bromide – CTAB) in the second stage on forming core-shell structured silica nanoparticles. Transmission electron microscopy (TEM) characterization showed that no core-shell structure formed when no surfactant was used, and the coating mechanism was clearly explained. SSN@CTAB-SSN particles were about 160.6 ± 0.8 nm, with the shell having a size of about 60 nm. The zeta potential and stability were measured by dynamic light scattering (DLS), which was $+31.5 \pm 0.7$ mV.

Keywords: Core-shell structure, CTAB, HMSN, particle size, surfactant, TEOS.

1. INTRODUCTION

In recent years, nanomaterials have attracted the attention of scientists because of their unique properties compared to the original bulk materials. Silica nanomaterials hold an important position and are widely used in many different industrial applications, such as electronics, aerospace, catalysis, and pharmaceuticals [1, 2]. Especially, hollow mesoporous silica nanoparticles (HMSN) have attracted the attention of many scientists. HMSN has a capillary structure similar to MSN and internal pores, so it can contain more drug molecules, minimizing the possibility of foreign material accumulation in the body, thus promising the potential to replace MSN materials in the future.

HMSN can be synthesized by many different methods, such as soft-template, self-template; a hard template is a popular method nowadays because it can control the granulation process and particle size [3]. Current studies only focus on the synthesis process, surface modification of the resulting materials, and their applications in various fields. Meanwhile, the silica nanoparticles formed in each stage have not been thoroughly studied and clearly explained. Especially, the stage of synthesizing core-shell structured silica nanoparticles is the stage that directly affects the results of hollow-structured nanoparticles.

Surfactants play a vital role in this stage. Surfactants (based on the charge of the head groups) are classified as nonionic, anionic, cationic, and zwitterionic (carrying both positive

and negative charges) surfactants. Some typical surfactants that have been used for the synthesis of nanoparticles are cetyl trimethyl ammonium bromide (CTAB), which is a cationic surfactant, dioctylsulfosuccinate sodium (AOT), which is an anionic surfactant, phosphatidylcholine (PC), which is an amphoteric surfactant, and Triton X-100, which is nonionic [4]. These surfactant molecules adsorb at the interfaces (boundaries between two immiscible phases) and are used to stabilize microemulsions by reducing surface tension and free energy [5]. Another characteristic of surfactants is their tendency to aggregate to form micelles at a specific concentration, called the critical micelle concentration (CMC)—these micelles serve as templates for the condensed silica precursors.

In this study, the influence of surfactant on the formation of core-shell structured silica nanoparticles was investigated. The obtained products were characterized by a set of experiments, including TEM, TGA, BET, and zeta potential.

2. MATERIALS AND METHODS

2.1. Materials

Tetraethyl orthosilicate (TEOS, 98%) was obtained from Sigma, cetyltrimethyl-ammonium bromide (CTAB, 99%), and ammonia solution (NH$_3$ (aq), 28%) were obtained from Merck, and ethanol ($\geq$ 99.9%) was purchased from Prolabo. All chemicals were of reagent grade and used without further purification.

2.2. Synthesis of solid silica nanoparticles (SSN)

Solid silica nanoparticles (SSN) were synthesized using the Stober method. The concentration of reactants was carried out according to the group's previously reported research [2]. A mixture of Ethanol (13.5 M), deionized water (deH$_2$O) (6.0 M), and NH$_3$ (0.38 M) was stirred for 30 minutes at 50 °C. Then, TEOS solution (0.29 M) was added to the mixture, and the reaction was carried out for 6 hours. The obtained product was membrane dialyzed (MWCO 12-14 KDa) in deionized water. Finally, SSN was freeze-dried.

2.3. Synthesis of core-shell structured silica nanoparticles

The synthesis of core-shell silica nanoparticles was carried out by the sol-gel method using TEOS as a silica-containing precursor [6]. This is a typical method for synthesizing mesoporous silica nanoparticles, such as M41S, MCM-41, and MCM-48, resulting in a mesoporous shell structure.

To coat the mesoporous silica nanoshell on the SSN particles, the ratio of reactants was based on the group's published mesoporous silica nanoparticle synthesis process and was adjusted to suit the amount of SSN solid silica nanoparticle used [7-9].

Solid silica nanoparticles (SSN) were dispersed in deH$_2$O and stirred with a surfactant solution for 30 minutes at 50°C. After that, an ethanol solution and NH$_3$ were added to the mixture (1.43:0.05, M/M), and TEOS (0.27 mol/L) was added last. Continue stirring for 6 hours at 50°C. The product was dialyzed with a 12-14 KDa cellulose membrane in deH$_2$O for about 4 days in deionized water, changing water four times/day, and then freeze-dried to obtain the sample. The effect of surfactant was performed under two conditions: no surfactant was used, and the surfactant (Cetyltrimethylammonium Bromide - CTAB 0.05 mol/L), shown in Figure 1. The corresponding sample symbols were SSN-SSN and SSN@CTAB/SSN.
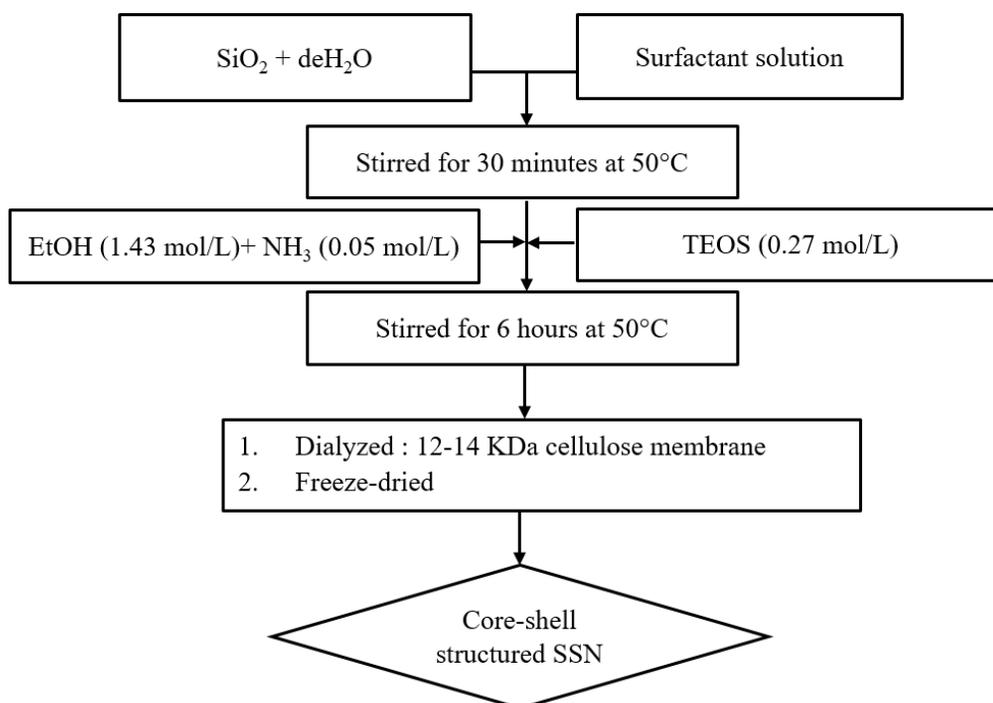
```
┌─────────────────────────┐        ┌─────────────────────────┐
│   SiO₂ + deH₂O          │        │   Surfactant solution   │
└─────────────────────────┘        └─────────────────────────┘
```

$SiO_2 + deH_2O$ / Surfactant solution

Stirred for 30 minutes at 50°C

EtOH (1.43 mol/L)+ NH$_3$ (0.05 mol/L) ← TEOS (0.27 mol/L)

Stirred for 6 hours at 50°C

1. Dialyzed : 12-14 KDa cellulose membrane
2. Freeze-dried

Core-shell structured SSN

Figure 1. Schematic of core-shell structured silica nanoparticles synthesis

2.4. Characterization

The morphology of the material was examined by transmission electron microscopy (TEM), performed at an accelerating voltage of 100 kV on JEM-1400 equipment.

Particle size and zeta potential were evaluated through a dynamic light scattering method using a Nano SZ 100 particle size measuring device (SZ-100, Horiba, Kyoto, Japan). In addition, based on TEM images and using ImageJ software to count the particle sizes, combined with Origin software, the average particle size and particle size distribution can be calculated.

Thermal gravimetric analysis (TGA) was performed with a TGAnalyzer (Mettler Toledo, OH, USA) under a nitrogen flow. The heating rate was set at 10 ºC per minute, and the temperature ranged from 25 °C to 800 ºC.

The surface area was evaluated using the N_2 adsorption-desorption method at 77 K on Tristar Micromeritics 3000 equipment.

3. RESULTS AND DISCUSSION

3.1. Results of synthesis of solid silica nanoparticles (SSN)

According to the Stober method, the SSN formed was amorphous [10]. The SSN particles had a size of 133.2 ± 1.7 nm and a narrow particle size distribution according to the DLS dynamic light scattering method (Figure 2a'). On the other hand, the SSN was observed by transmission electron microscopy (TEM) to examine the morphology and size, as shown in Figure 2a. The findings demonstrated the spherical shape and respectable high homogeneity of SSN. According to the size statistics from the TEM images, the SSN had a size of 104.0 ± 0.7 nm [9]. The particle size observed by electron microscopy was usually smaller than the hydrodynamic diameter measured by DLS due to the loss of the hydrate layer when the sample

was dried [11]. The zeta potential of SSN is -42.9 ± 1.4 mV; the SSN nanoparticles are negatively charged due to the dissociation of the silanol group (Si–OH) on the surface in Figure 2a".
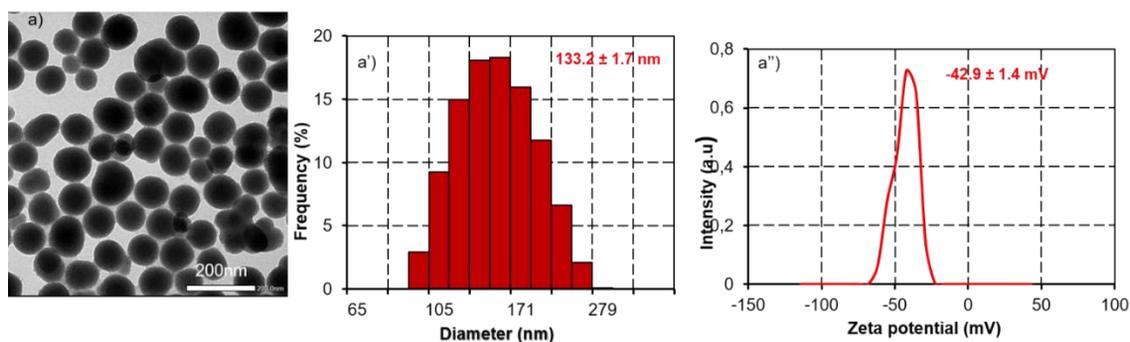

Figure 2. TEM images (a), size distribution histograms (a') from DLS data of SSN, and zeta potentials of SSN (a'')

3.2. Effect of surfactant in synthesizing core-shell silica nanoparticles

TEM image results in Figure 3a show that the SSN-SSN particles are spherical, but no core-shell structure is formed when no surfactant is used. Thus, in the absence of a CTAB surfactant, the coating process occurs similarly to the Stober method mechanism, including hydrolysis and condensation of TEOS on solid SSN particles. The SSN-SSN are 173.7 ± 1.3 nm, larger than the original SSN particles.
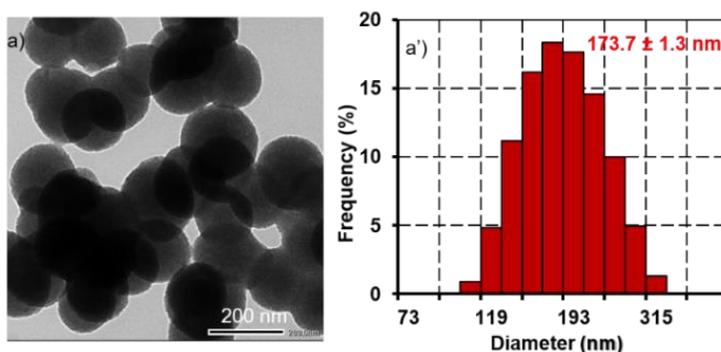

Figure 3. TEM images (a) and size distribution histograms (a') from DLS data of SSN-SSN

Based on Figure 4a, it can be seen that SSN@CTAB-SSN has a spherical shape like the original SSN solid nano silica core. The silica shell on the core is formed by the hydrolysis and condensation reaction of TEOS in the presence of CTAB. The resulting silica nanoparticles have a core-shell structure when using CTAB surfactant. This is shown in the high-magnification cross-section of a silica nanoparticle, corresponding to the core's dark black part inside and the shell's lighter black part [12]. The SSN@CTAB-SSN particles were larger than the SSN-SSN particles, about 205.8 ± 5.9 nm, and had a high polydispersity index (PDI) of 0.091 (Figure 4a'') due to the presence of CTAB. This result is consistent with the study of Wei Wang et al., especially since the particle size will increase with increasing CTAB concentration [13]. Observe Figure 4a', the size of SSN@CTAB-SSN particles is about 160.6 ± 0.8 nm (according to statistics from TEM images), so the shell will have a size of about 60 nm. Thus, CTAB plays an important role in successfully coating the shell and orienting its shape and structure.
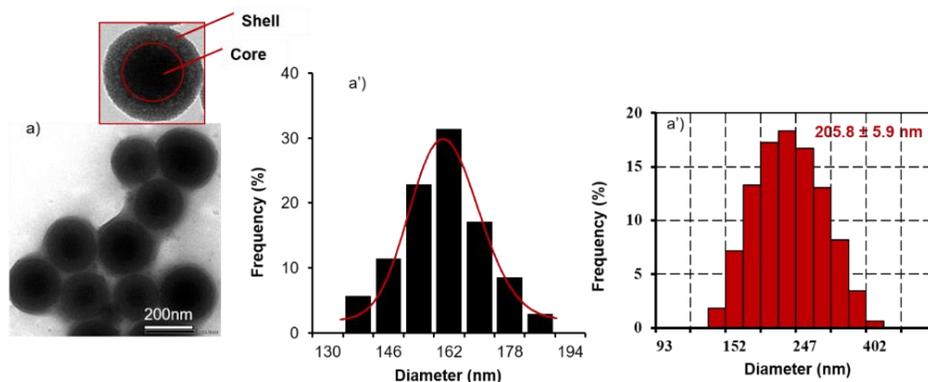
Figure 4. TEM images (a) and size distribution histograms (a') from TEM imaging and (a'')
from DLS data of SSN@CTAB-SSN

Several studies have reported the critical micelle concentration (CMC) of CTAB to be 1 mM by K. Eskilsson [14] and 0.89 mM by A. Modaressi [15]. In addition, Gao et al. concluded that 0.92 mM [16] or 0.8 mM by Maiti [17]. Free micelles will form when the CTAB concentration is much larger than the CMC value. When the nanoparticles approach each other in the presence of free micelles, the hydrocarbon chains in the micelles will leave voids, creating a solvent reservoir. As the particles get closer to each other, the solvent between the particles diffuses out to reduce the concentration gradient, creating osmotic pressure and causing the particles to aggregate together [18, 19]. The coating process aimed to create complete micelles, so the CTAB concentration used was 50 mM, much larger than the CMC value of CTAB. Therefore, observing Figure 5, it can be seen that the SSN@CTAB-SSN particles aggregated together (Figure 5a), and after being dialyzed with cellulose membrane with distilled water to remove excess CTAB, the particles no longer agglomerated (Figure 5a').
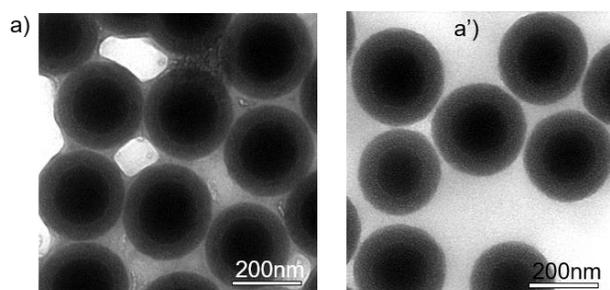

Figure 5. TEM images of SSN@CTAB-SSN before and after dialysis with cellulose
membrane with distilled water (a, a')

3.3. The role of CTAB in the synthesis of core-shell structured silica nanoparticles

The synthesis of core-shell structured nanoparticles with CTAB surfactant is similar to the synthesis mechanism of the MCM-41 of mesoporous silica nanoparticles. Studies on the synthesis of mesoporous silica nanoparticles have concluded that there are two different mechanisms: (i) First, the surfactant at high concentrations self-assembles into a lyotropic crystalline phase (or micelles), and these micelles aggregate together to form micelle templates. This is followed by the condensation of silica around the micelle templates. (ii) The second mechanism can also form micelles but at lower surfactant concentrations; the self-aggregation of surfactant and silica is shaped by a silica-containing precursor solution (possibly TEOS) to form a hexagonal, cubic, or plate-shaped liquid crystalline phase [20]. The

CTAB surfactant has long hydrophobic alkyl chains, so these alkyl chains will aggregate together to reduce the interaction energy of the non-polar alkyl ends with the highly polar water solvent molecules. The result is the formation of micelles, which have a hydrophobic core containing long alkyl chains and a hydrophilic surface due to the ionic character of the ammonium groups with the positively charged CTA+ ends. Most of the micelles formed are spherical because, in this geometry, the surface energy is most effectively reduced. Furthermore, the spherical shape allows the formation of more micelles from a given amount of starting material. However, the shape of the micelles formed depends on the surfactant concentration. Therefore, the initial spherical micelles gradually transform into long tubes, and then the same tubes aggregate to form a hexagonal structure according to mechanism 1 (Figure 6a) or also form a hexagonal micelle template according to mechanism 2, which is the template for the structure of MCM-41 material [21, 22]. These micelles are adsorbed on the surface of the SSN solid silica nanocore by the electrostatic interaction between the CTA+ head and the negatively charged surface of the SSN solid core [23, 24] as shown in Figure 6a'. Finally, the hydrolysis of the added TEOS forms silicic acid; in the supersaturated state, the negatively charged surface of the silicic acid will condense on the surface around the core-micelle template to form a silica shell, as shown in Figure 6a''.
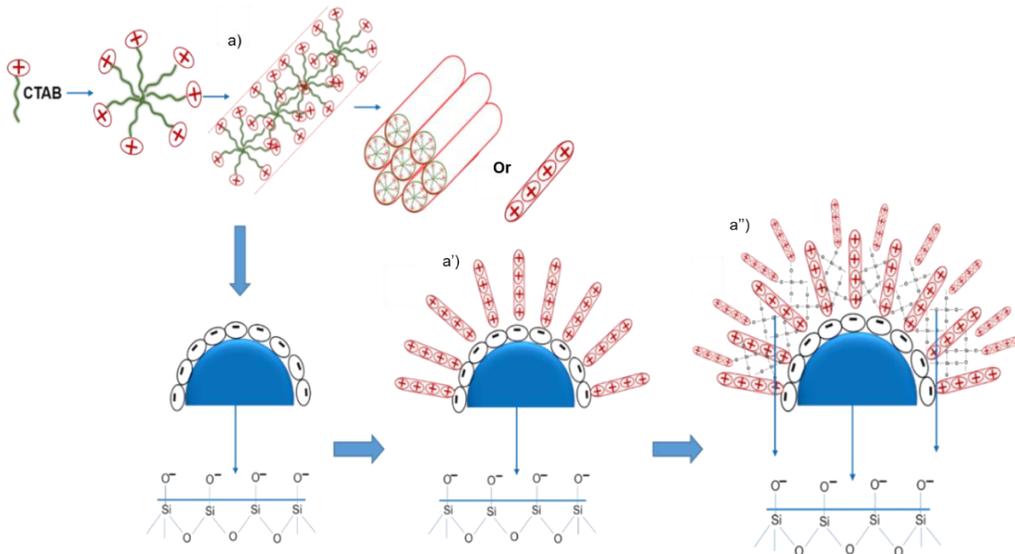

Figure 6. In the process of forming micelles (a), the electrostatic interaction between the CTA+ tip and the negatively charged surface (a')
and the silicic acid will condense on the surface around the core – micelles (a'')

3.4. The characterization of SSN@CTAB-SSN

The surface charge of core-shell structured silica nanoparticles was positive at +31.5 ± 0.7 mV, indicating a charge reversal on the surface compared to SSN (Figure 7). This is due to the surface charge being completely shielded by the adsorption of CTAB with the positively charged group CTA+, resulting in a sign reversal of the surface potential [23, 25]. This result is consistent with previous studies on the surface interaction of silica colloids SiO_2, with the addition of cationic surfactants [26, 27]. SSN@CTAB-SSN silica nanoparticles with zeta potential values greater than 30 mV indicate the formation of a bilayer of CTAB molecules at the silica surface [28, 29]. Thus, the change in zeta potential value proves that the shell layer has been successfully coated on the SSN solid core.
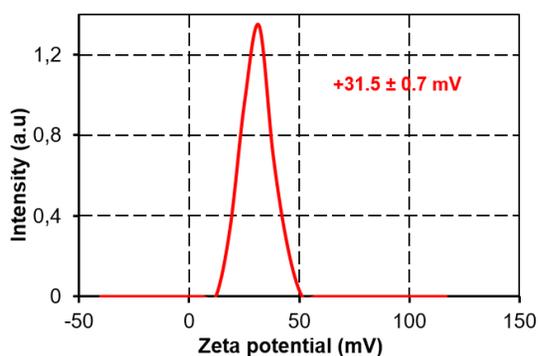
Figure 7. Zeta potentials of SSN@CTAB-SSN

The zeta potential value in the solution over time from 0 to 48 hours tends to decrease in the first 6 hours; after that, the zeta potential changes insignificantly, proving that the system is stable. In addition, actual observation shows that the solution at 48 hours is still opaque white. There is no separation of SSN@CTAB-SSN particles, and there are a few particles at the bottom of the solution container, as shown in Figure 8.
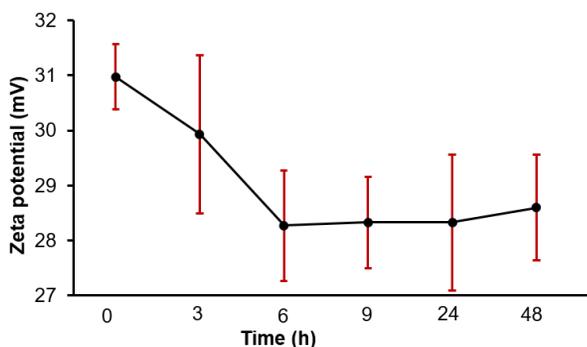

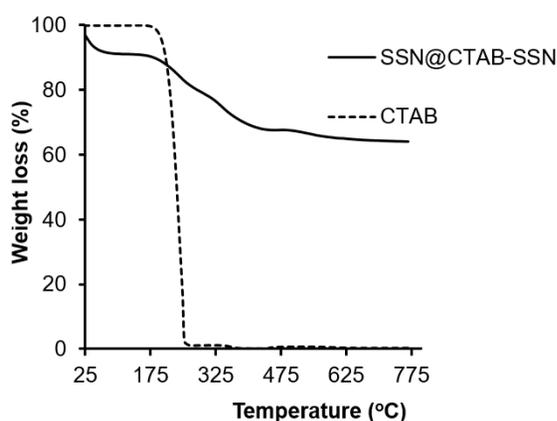*Figure 8.* Zeta potential of SSN@CTAB-SSN in solutions for 48h

Figure 9. Thermogravimetric analysis for SSN@CTAB-SSN (solid line), and CTAB (dashed line)

In addition, to determine the amount of CTAB contained in the SSN@CTAB-SSN sample, a thermogravimetric analysis method will be used [22]. The TGA curve of

SSN@CTAB-SSN particles is shown in Figure 9. The sample calcination process was carried out from 25 $^{\circ}$C to 800 $^{\circ}$C at a rate of 10 $^{\circ}$C/min. The weight loss of the analyzed sample increased with increasing treatment temperature, similar to the thermal analysis results for the SSN sample.

At temperatures < 170 $^{\circ}$C, the corresponding weight loss is about 9% due to the evaporation of physically adsorbed water and partial dehydroxylation of silanol groups on the material surface. At temperatures from 200 $^{\circ}$C to 300 $^{\circ}$C, the weight loss is 10%. Of these, 3% of the weight is due to the evaporation of physically bound water and partial dehydroxylation of silanol groups inside the material structure, and organic impurities from the original material. Thus, about 7% of CTAB is contained in the SSN@CTAB-SSN sample.

The surface area of SSN@CTAB-SSN particles was determined by the N_2 gas adsorption-desorption method (using the BET equation), with a surface area of 46.6 m^2/g. According to the IUPAC classification, the adsorption-desorption isotherm type belongs to type II, and the material has no capillary structure (Figure 10).
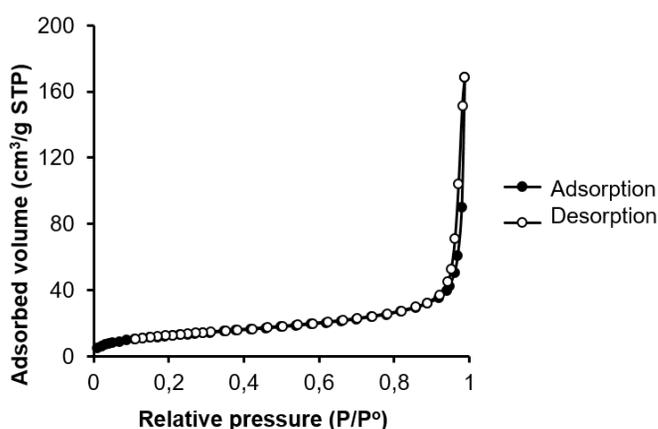

Figure 10. Nitrogen adsorption-desorption isotherms of SSN@CTAB-SSN

4. CONCLUSION

The impact of the surfactant on the synthesis of core-shell silica nanoparticles was examined. The formation of the core-shell structure is contingent upon the presence of surfactants. The effective synthesis of SSN@CTAB-SSN particles, measuring 160.6 ± 0.8 nm, exhibited a spherical morphology and good uniformity. The mechanism of the shell coating process was elucidated, highlighting the crucial role of CTAB in stabilizing and orienting the shell structure. Furthermore, the zeta potential of SSN@CTAB-SSN was +31.5 ± 0.7 mV, and the surface area was 46.6 m^2/g.

Acknowledgement

REFERENCES

1. Rahman, I. A., Vejayakumaran, P., Sipaut, C. S., Ismail, J., Bakar, M. A., Adnan, R., & Chee, C. K. - An optimized sol–gel synthesis of stable primary equivalent silica

particles. Colloids and Surfaces A: Physicochemical and Engineering Aspects **294** (1-3) (2007) 102-110. https://doi.org/10.1016/j.colsurfa.2006.08.001

2. Nguyen, T. N. T., Nguyen-Tran, D. H., Bach, L. G., Du Truong, T. H., Le, N. T. T., & Nguyen, D. H. - Surface PEGylation of hollow mesoporous silica nanoparticles via aminated intermediate. - Progress in Natural Science: Materials International **29** (6) (2019) 612-616. https://doi.org/10.1016/j.pnsc.2019.10.002

3. Shi, S., Chen, F., & Cai, W. - Biomedical applications of functionalized hollow mesoporous silica nanoparticles: focusing on molecular imaging. Nanomedicine **8** (12) (2013) 2027-2039. DOI: 10.2217/nnm.13.177

4. Soleimani Zohr Shiri, M., Henderson, W., & Mucalo, M. R. - A review of the lesser-studied microemulsion-based synthesis methodologies used for preparing nanoparticle systems of the noble metals, Os, Re, Ir and Rh. Materials **12** (12) (2019) 1896. https://doi.org/10.3390/ma12121896

5. Hussain, T., & Batool, R. - Microemulsion route for the synthesis of nano-structured catalytic materials. In: Karunaratne, D. N., Pamunuwa, G., & Ranatunga, U. (Eds). Properties and Uses of Microemulsions Properties and uses of microemulsions. IntechOpen, 2017. http://dx.doi.org/10.5772/66183

6. Vazquez, N. I., Gonzalez, Z., Ferrari, B., & Castro, Y. - Synthesis of mesoporous silica nanoparticles by sol–gel as nanocontainer for future drug delivery applications. Boletín de la Sociedad Española de Cerámica y Vidrio **56** (3) (2017) 139-145. https://doi.org/10.1016/j.bsecv.2017.03.002.

7. Thi, T. T. N., Tran, T. V., Tran, N. Q., Nguyen, C. K., & Nguyen, D. H. - Hierarchical self-assembly of heparin-PEG end-capped porous silica as a redox sensitive nanocarrier for doxorubicin delivery. Materials Science and Engineering: C **70** (2017) 947-954. https://doi.org/10.1016/j.msec.2016.04.085

8. Vo, U.V., Tran, T.V., Nguyen, D. M. T., Nguyen, C. K., Nguyen, T. N. T & Nguyen, D. H. - Effective pH-responsive hydrazine-modified silica for doxorubicin delivery. Asian Journal of Medicine and Health **4** (1) (2017) 1-7. https://doi.org/10.9734/AJMAH/2017/32253

9. Nguyen-Thi, N. T., Pham Tran, L. P., Le, N. T. T., Cao, M. T., Tran, T. N., Nguyen, N. T., ... & Trung, N. Q. - The engineering of porous silica and hollow silica nanoparticles to enhance drug-loading capacity. Processes **7** (11) (2019) 805. https://doi.org/10.3390/pr7110805

10. De Keizer, A., Van der Ent, E. M., & Koopal, L. K. - Surface and volume charge densities of monodisperse porous silicas. Colloids and Surfaces A: Physicochemical and Engineering Aspects **142** (2-3) (1998) 303-313. https://doi.org/10.1016/S0927-7757(98)00268-4

11. Kobler, J., Möller, K., & Bein, T. - Colloidal suspensions of functionalized mesoporous silica nanoparticles. ACS Nano **2** (4) (2008) 791-799. https://doi.org/10.1021/nn700008s

12. Chen, F., Hong, H., Shi, S., Goel, S., Valdovinos, H. F., Hernandez, R., ... & Cai, W. - Engineering of hollow mesoporous silica nanoparticles for remarkably enhanced tumor active targeting efficacy. Scientific Reports **4** (1) (2014) 5080. https://doi.org/10.1038/srep05080

13. Wang, W., Gu, B., Liang, L., & Hamilton, W. A. - Adsorption and structural arrangement of cetyltrimethylammonium cations at the silica nanoparticle− water

interface. The Journal of Physical Chemistry B **108** (45) (2004) 17477-17483. https://doi.org/10.1021/jp048325f

14. Eskilsson, K., & Yaminsky, V. V. - Deposition of monolayers by retraction from solution: ellipsometric study of cetyltrimethylammonium bromide adsorption at silica− air and silica− water interfaces. Langmuir **14** (9) (1998) 2444-2450. https://doi.org/10.1021/la971066j

15. Modaressi, A., Sifaoui, H., Grzesiak, B., Solimando, R., Domanska, U., & Rogalski, M. - CTAB aggregation in aqueous solutions of ammonium based ionic liquids; conductimetric studies. Colloids and Surfaces A: Physicochemical and Engineering Aspects **296** (1-3) (2007) 104-108. https://doi.org/10.1016/j.colsurfa.2006.09.031.

16. Gao, H., Zhu, R., Yang, X., Mao, S., Zhao, S., Yu, J., & Du, Y. - Properties of polyethylene glycol (23) lauryl ether with cetyltrimethylammonium bromide in mixed aqueous solutions studied by self-diffusion coefficient NMR. Journal of Colloid and Interface Science **273** (2) (2004) 626-631. https://doi.org/10.1016/j.jcis.2003.12.047

17. Maiti, P. K., Kremer, K., Flimm, O., Chowdhury, D., & Stauffer, D. - Cross-linking of micelles by gemini surfactants. Langmuir **16** (8) (2000) 3784-3790. https://doi.org/10.1021/la9914458

18. Furusawa, K., Sato, A., Shirai, J., & Nashima, T. - Depletion flocculation of latex dispersion in ionic micellar systems. Journal of Colloid and Interface Science **253** (2) (2002) 273-278. https://doi.org/10.1006/jcis.2002.8515

19. Shi, J. - Oxide nanoparticles and nanostructured coatings by wet chemical processing (Doctoral Dissertation, Ohio State University). OhioLINK Electronic Theses and Dissertations Center, 2006. http://rave.ohiolink.edu/etdc/view?acc_num=osu1148318139

20. Lyabode Akinjokun, A., & Ogunfowokan, A. O. - Biomass, Abundant Resources for Synthesis of Mesoporous Silica Material. In: Microporous and mesoporous materials, IntechOpen (2016). http://dx.doi.org/10.5772/63463

21. Rath, D., Rana, S., & Parida, K. M. - Organic amine-functionalized silica-based mesoporous materials: an update of syntheses and catalytic applications. RSC Advances **4** (100) (2014) 57111-57124. https://doi.org/10.1039/C4RA08005J

22. Sadasivan, S., Fowler, C. E., Khushalani, D., & Mann, S. - Nucleation of MCM-41 Nanoparticles by Internal Reorganization of Disordered and Nematic-Like Silica–Surfactant Clusters. Angewandte Chemie **114** (12) (2002) 2255-2257. https://doi.org/10.1002/1521-3773(20020617)41:12<2151::AID ANIE2151>3.0.CO;2-U

23. Lelong, G., Bhattacharyya, S., Kline, S., Cacciaguerra, T., Gonzalez, M. A., & Saboungi, M. L. - Effect of surfactant concentration on the morphology and texture of MCM-41 materials. The Journal of Physical Chemistry C **112** (29) (2008) 10674-10680. https://doi.org/10.1021/jp800898n

24. Henry, B. S. -Control of mesostructured silica particle morphology. Journal of Materials Chemistry **11** (3) (2001) 951-957. https://doi.org/10.1039/B005713O

25. Fuglestad, B., Gupta, K., Wand, A. J., & Sharp, K. A. - Characterization of cetyltrimethylammonium bromide/hexanol reverse micelles by experimentally benchmarked molecular dynamics simulations. Langmuir **32** (7) (2016) 1674-1684. https://doi.org/10.1021/acs.langmuir.5b03981

26. Esumi, K. - Interactions between surfactants and particles: dispersion, surface modification, and adsolubilization. Journal of Colloid and Interface Science **241** (1) (2001) 1-17. https://doi.org/10.1006/jcis.2001.7740

27. Goloub, T. P., Koopal, L. K., Bijsterbosch, B. H., & Sidorova, M. P. - Adsorption of cationic surfactants on silica. Surface charge effects. Langmuir **12** (13) (1996) 3188-3194. https://doi.org/10.1021/la9505475

28. Liu, Y., Tourbin, M., Lachaize, S., & Guiraud, P. - Silica nanoparticles separation from water: Aggregation by cetyltrimethylammonium bromide (CTAB). Chemosphere **92** (6) (2013) 681-687. https://doi.org/10.1016/j.chemosphere.2013.03.048

29. Bryleva, E. Y., Vodolazkaya, N. A., Mchedlov-Petrossyan, N. O., Samokhina, L. V., Matveevskaya, N. A., & Tolmachev, A. V. - Interfacial properties of cetyltrimethylammonium-coated SiO₂ nanoparticles in aqueous media as studied by using different indicator dyes. Journal of colloid and interface science, **316** (2) (2007) 712-722. https://doi.org/10.1016/j.jcis.2007.07.036

TÓM TẮT

ẢNH HƯỞNG CỦA CHẤT HOẠT ĐỘNG BỀ MẶT ĐẾN QUÁ TRÌNH TỔNG HỢP HẠT NANO SILICA CẤU TRÚC LÕI - VỎ

Nguyễn Thị Ngọc Huyền[1], Nguyễn Xuân Thị Diễm Trinh[1], Nguyễn Minh Thảo[2],

Nguyễn Thị Ngọc Trăm[1,*]

[1]*Trường Y Dược, Trường Đại học Trà Vinh, Việt Nam*

[2]*Phòng Khoa học Công nghệ, Trường Đại học Đồng Tháp, Việt Nam*

[*]*Email: tram06@tvu.edu.vn*

Nano silica cấu trúc rỗng - HMSN được tổng hợp bằng phương pháp khuôn cứng gồm 3 giai đoạn: Tổng hợp lõi nano silica rắn (SSN), hạt nano cấu trúc lõi - vỏ (SSN@CTAB-SSN) và ăn mòn lõi tạo thành nano silica rỗng. Trong nghiên cứu này thực hiện đánh giá ảnh hưởng của chất hoạt động bề mặt đến quá trình tạo thành hạt nano cấu trúc lõi - vỏ. Kết quả ảnh TEM cho thấy không có cấu trúc lõi - vỏ tạo thành khi không sử dụng chất hoạt động bề mặt, ngoài ra cơ chế quá trình phủ lớp vỏ được giải thích một cách rõ ràng. Các hạt SSN@CTAB-SSN có kích thước khoảng 160,6 ± 0,8 nm, với vỏ có kích thước khoảng 60 nm. Độ bền của các hạt theo thời gian được đánh giá bằng phương pháp tán xạ ánh sáng động (DLS), thế zeta của các hạt SSN@CTAB-SSN là +31,5 ± 0,7 mV.

Từ khoá: Cấu trúc lõi-vỏ, CTAB, HMSN, kích thước hạt, chất hoạt động bề mặt, TEOS.